THE JOURNAL OF BIOLOGICAL CHEMISTRY VOL. 290, NO. 11, pp. 6975–6985, March 13, 2015

Exposure of Neutralizing Epitopes in the Carboxyl-terminal Domain of TcdB Is Altered by a Proximal Hypervariable Region*

Received for publication, September 16, 2014, and in revised form, January 19, 2015 Published, JBC Papers in Press, January 22, 2015, DOI 10.1074/jbc.M114.612184

Jason L. Larabee, Aleze Krumholz, Jonathan J. Hunt, Jordi M. Lanis, and Jimmy D. Ballard[1]

From the Department of Microbiology and Immunology, University of Oklahoma Health Sciences Center, Oklahoma City, Oklahoma 73104

Background: TcdB from 027 strains is not as sensitive to antibody neutralization as TcdB from 012 strains, although neutralizing epitopes are present on both forms.
Results: Sequence alterations in strain-specific TcdB influence intramolecular protein-protein interactions and exposure of neutralizing epitopes.
Conclusion: Our work uncovers a mechanism used by TcdB to shield neutralizing epitopes.
Significance: This study demonstrates how strain-specific TcdB can avoid antibody targeting.

The sequence, activity, and antigenicity of TcdB varies between different strains of *Clostridium difficile*. As a result, ribotype-specific forms of TcdB exhibit different toxicities and are not strongly cross-neutralized. Using a combination of biochemical and immunological approaches, we compared two important variants of TcdB ($TcdB_{012}$ and $TcdB_{027}$) to identify the mechanisms through which sequence differences alter epitopes and activity of the toxin. These analyses led to the discovery of a critical variation in the 1753–1851 (B2′) region of TcdB, which affects the exposure of neutralizing epitopes in the toxin. Sequence comparisons found that the B2′ region exhibits only 77% identity and is the most variable sequence between the two forms of TcdB. A combination of biochemical, analytical, and mutagenesis experiments revealed that the B2′ region promotes protein-protein interactions. These interactions appear to shield neutralizing epitopes that would otherwise be exposed in the toxin, an event found to be less prominent in $TcdB_{012}$ due to sequence differences in the 1773–1780 and 1791–1798 regions of the B2′ domain. When the carboxyl-terminal domains of $TcdB_{012}$ and $TcdB_{027}$ are swapped, neutralization experiments suggest that the amino terminus of TcdB interacts with the B2′ region and impacts the exposure of neutralizing epitopes in the carboxyl terminus. Collectively, these data suggest that variations in the B2′ region affect protein-protein interactions within TcdB and that these interactions influence the exposure of neutralizing epitopes.

Clostridium difficile TcdB[2] (~269 kDa) is an enzymatic bacterial toxin that glucosylates Rho, Rac, and Cdc42 following entry into the cytosol of cells (1). TcdB is expressed by disease-causing strains of *C. difficile*, is essential to *C. difficile* infection (CDI), and is capable of recapitulating many aspects of CDI (2–6). Studies focused on TcdB have provided insight into *C. difficile* pathogenesis, and findings suggest that blocking this toxin could ameliorate disease.

TcdB (2366 residues) enters cells by receptor-mediated endocytosis and translocates into the cytosol following acidification of the endosome (7–10). TcdB undergoes acid pH-induced conformational changes within the endosome and, using a mechanism reminiscent of diphtheria toxin, inserts into the membrane with its pore-forming domain (residues 1035–1107) (11). The steps following insertion into the membrane and translocation into the cytosol have not been described, but the glucosyltransferase domain (GTD; residues 1–543) is known to be released into the cytosol following autoprocessing by the proximal cysteine protease domain (CPD; residues 554–767) (12, 13). The GTD and CPD appear to be reasonable drug targets, but recent reports indicate that TcdB mutants lacking these activities remain cytotoxic (14–16). This raises the possibility that the toxin has other, yet undefined, intracellular activities, and two recent reports found that TcdB modulates the NADPH oxidase complex and causes pyknosis in the absence of glucosyltransferase activity (15, 17). Thus, vaccination and other strategies to block earlier steps in cellular intoxication, such as cell binding, may be needed to prevent all of the known and unknown intracellular activities of TcdB.

Development of TcdB-targeted vaccines or therapeutic antibodies for treating most cases of CDI faces an important obstacle; strain type-specific forms of TcdB vary in sequence, toxicity, and antigenicity (18–22). Earlier findings from our group suggested that conformational variations may influence the differences in toxicity between the two forms of TcdB. For example, experiments found that TcdB produced by the hypervirulent *C. difficile* 027 ribotype ($TcdB_{027}$) undergoes unfolding and exposure of hydrophobic domains at a higher acidic pH than TcdB produced by the less virulent *C. difficile* ribotype (termed $TcdB_{012}$ herein and representative of several histor-

* This work was supported, in whole or in part, by National Institutes of Health Grant R01HL084489 (to J. D. B.).
[1] To whom correspondence should be addressed: University of Oklahoma Health Sciences Center, Department of Microbiology and Immunology, BMSB: 1053, 940 Stanton L. Young Blvd., Oklahoma City, OK 73104. Tel.: 405-271-3855; E-mail: jimmy-ballard@ouhsc.edu.
[2] The abbreviations used are: TcdB, *C. difficile* toxin B; CDI, *C. difficile* infection; GTD, glucosyltransferase domain; CPD, cysteine protease domain; GF, gel filtration; BS^3, bis(sulfosuccinimidyl) suberate; AGE, agarose gel electrophoresis.

ical ribotypes, such as 001, 003, 012, and 087) (22). Studies have also shown $TcdB_{027}$, but not $TcdB_{012}$, adopts a structure where the CPD is occluded from external labeling by a substrate-based fluorescent probe (21). This conformational difference corresponds with more efficient autoprocessing by $TcdB_{027}$. As a result, $TcdB_{027}$ appears to intoxicate cells more efficiently than $TcdB_{012}$ (21, 22). Corresponding to the sequence differences and possible variations in structure, we also reported that rabbit polyclonal antisera recognizing the carboxyl-terminal domains (residues 1652–2366) of $TcdB_{027}$ and $TcdB_{012}$ do not strongly cross-neutralize (20). However, the extent to which substantial conformational differences, rather than more subtle sequence variation in specific epitopes, limits cross-neutralization is not known.

In the current study, we show that the carboxyl-terminal domain of $TcdB_{027}$ is prone to intermolecular interactions and forms a higher order complex, which precludes the exposure of neutralizing epitopes through a process we termed "epitope cloaking." Cloaking appears to require a distinct 98-residue domain, which exhibits only 77% identity between the two forms of the toxin. These findings support a model in which $TcdB_{027}$ exists in a conformation that can both impact toxicity and the exposure of neutralizing epitopes.

EXPERIMENTAL PROCEDURES

Production of Native and Recombinant TcdB—Native TcdB was produced by culturing *C. difficile* (VPI 10463 or NAP1/BI/027) with the dialysis method as described previously (22). From these cultures, supernatants were isolated, and TcdA was removed by a thyroglobulin affinity chromatography protocol. After removing TcdA, TcdB was purified using anion exchange (Q-Sepharose) chromatography in 20 mM Tris-HCl, pH 8.0, and 20 mM $CaCl_2$. This method yields pure native TcdB, as demonstrated by a single 270 kDa band when analyzed by SDS-PAGE.

Recombinant TcdB was expressed and purified in a *Bacillus megaterium* system (MoBiTec, Göttingen, Germany) as described previously by others (23). The $tcdB_{027}$ gene was amplified from *C. difficile* genomic DNA and cloned into the *B. megaterium* expression plasmid (pC-His1622) between the BsrGI and NgoMIV restriction sites. The $tcdB_{012}$ gene in pC-His1622 was a gift from B. Lacy. Hybrid forms of TcdB were generated where the carboxyl terminus (amino acids 1668–2366) of each toxin was swapped. This resulted in $TcdB_{012}$ that had the carboxyl terminus from $TcdB_{027}$ ($TcdB_{012}$/B2′$B3_{027}$) and $TcdB_{027}$ that had the carboxyl terminus from $TcdB_{012}$ ($TcdB_{027}$/B2′$B3_{012}$). To perform this switch, a BspEI site was engineered into both the $tcdB_{012}$ and $tcdB_{027}$ genes in the pC-His1622 plasmid. This BspEI site was created between nucleotides 4996 and 5001 by changing a single nucleotide with the QuikChange II XL site-directed mutagenesis kit (Agilent). This nucleotide substitution did not alter the amino acid sequence of either $TcdB_{012}$ or $TcdB_{027}$. After creating this restriction site, both $tcdB_{012}$ and $tcdB_{027}$ were digested with BsrGI and BspEI, which created a fragment containing the amino terminus of TcdB (amino acids 1–1667). $TcdB_{027}$/B2′$B3_{012}$ was generated when the segment of DNA containing the amino terminus of $TcdB_{027}$ was ligated into pC-His1622-$TcdB_{012}$ that had the amino terminus removed by digesting with BsrGI and BspEI. $TcdB_{012}$/B2′$B3_{027}$ was produced using a similar method. DNA sequencing was used to confirm the construction of $TcdB_{027}$/B2′$B3_{012}$ and $TcdB_{012}$/B2′$B3_{027}$.

To express recombinant TcdB, pC-His1622-TcdB was transformed into *B. megaterium* following the manufacturer's instructions (MoBiTec, Göttingen, Germany). After selecting for TcdB-positive clones, *B. megaterium* containing pC-His1622-TcdB was grown at 37 °C in LB medium supplemented with 10 μg/ml tetracycline. The culture were grown to an A_{600} of 0.3 and then induced for 5 h with 0.5% D-xylose. After induction, cells were isolated by centrifugation and resuspended in 20 mM HEPES (pH 8.0), 500 mM NaCl, and 20 mM imidazole. The cells were then lysed, and TcdB was purified by Ni^{2+} affinity chromatography. After elution, TcdB was buffer-exchanged into a storage buffer consisting of 20 mM HEPES (pH 8.0) and 500 mM NaCl. SDS-PAGE analysis of purity demonstrated that recombinant TcdB was ~90% pure.

Production of Recombinant GTD, B2′B3, and Mutant B2′B3—The B2′B3-encoding region of the *tcdB* gene (nucleotides 4961–7111; amino acids 1651–2366) from ribotype 012 or 027 was codon-optimized for *Escherichia coli* and cloned into pET15b expression plasmid (20). From these clones, PCR was used to amplify the regions encoding the B3 and the 1751–1852 fragment. These PCR products were cloned into the pENTR vector (Invitrogen) and transferred into expression vectors by a recombination reaction using LR Clonase (Invitrogen). The expression vectors used to express these carboxyl-terminal fragments were pET61Dest (EMD Millipore) and pDest17 (Invitrogen). The B2′B3 mutants described in the legend to Fig. 1 were generated in pET15b-B2′B3 using the QuikChange II XL site-directed mutagenesis kit (Agilent). To express and purify these proteins, *E. coli* (BL21 star DE3; Invitrogen) were transformed with pET15b-B2′B3, pET61Dest-B3, or pDest17–1752-1853. Then cultures of the transformed *E. coli* were grown to an A_{600} of 0.8 and induced with 300 μM isopropyl 1-thio-β-D-galactopyranoside for 16 h at 16 °C. These proteins were then purified by Ni^{2+} affinity chromatography and were ~90% pure as assessed by SDS-PAGE.

Recombinant GTD was produced by using PCR to amplify the regions encoding GTD from the $tcdB_{012}$ or $tcdB_{027}$ gene codon optimized for *E. coli*. These PCR products were cloned into the pENTR vector (Invitrogen) and transferred into the pDest15 (Invitrogen) expression vectors using LR Clonase (Invitrogen). The pDest15 vector allowed for the expression of the GTD with an amino-terminal GST tag in *E. coli*. After transforming the pDest15-GTD into *E. coli* (BL21 star DE3; Invitrogen), cultures were grown to an A_{600} of 0.8 and induced with 300 μM isopropyl 1-thio-β-D-galactopyranoside for 16 h at 16 °C. From these cultures, the GST fusion protein was isolated via affinity chromatography using glutathione-Superflow agarose (Pierce). SDS-PAGE was used to demonstrate that ~90% purity was achieved.

TcdB Neutralization Assays—These assays use the ability of TcdB to reduce CHO cell viability as a method to quantify TcdB neutralization. The antiserum used in these assays was produced by immunizing rabbits with B2′$B3_{012}$. In these experiments, CHO cells (ATCC) were cultured at 37 °C in the pres-

ence of 6% CO_2 with F12-K containing 10% FBS, 100 units/ml penicillin, and 100 μg/ml streptomycin. Prior to these assays, CHO cells were seeded in 96-well plates at a density of 1×10^4 cells/well and allowed to attach overnight. In these assays, TcdB was combined with a 1:100 dilution of serum in culture medium and incubated for 30 min before adding this mixture to cells. The toxin-exposed cells were incubated for 24 h, and cell viability was measured by the CCK-8 assay (Sigma), a WST-8 dye-based colorimetric reaction. In the blocking assays, the antiserum was incubated for 30 min with B2′B3, and then toxin was added. The incubation was continued for another 30 min, and then the incubation was added to CHO cells to assess neutralization. For examining the potential linear epitope (positions 1773–1780), this blocking assay was performed using a 19-amino acid peptide spanning residues 1769–1787 of $TcdB_{012}$. This peptide was synthesized and purified to 95% by GenScript (Piscataway, NJ).

Cross-linking—The B2′B3 or B3 fragment was cross-linked using bis(sulfosuccinimidyl) suberate (BS^3), which is a water-soluble homobifunctional cross-linking agent that reacts with primary amine groups. The cross-linking reaction was performed with 35 μM purified proteins and 700 μM BS^3 in a buffer consisting of 20 mM sodium phosphate (pH 7.2) and 500 mM NaCl. The reaction proceeded for 30 min at 25 °C and then was quenched with 40 mM Tris, pH 8.0.

Gel Filtration—To perform gel filtration, 300 μg of purified protein was loaded onto a Superose 6 10/300 GL column (GE Healthcare) at a flow rate of 250 μl/min. Chromatography was performed in a buffer consisting of 20 mM sodium phosphate (pH 7.2), 500 mM NaCl, and 2 mM DTT. Protein standards (Bio-Rad) were run under the same conditions in order to gauge the retention times of the proteins analyzed in these experiments.

Pull-down—In these experiments, 2 μM His-tagged B2′B3 was combined with 450 nM native TcdB (no tag) in 50 μl of a buffer consisting of 20 mM sodium phosphate (pH 7.2), 137 mM NaCl, and 0.01% Tween 20 (binding buffer). These proteins were incubated for 1 h at 37 °C, and then cobalt-coated magnetic beads (Dynabeads; Invitrogen) were added in order to isolate His-tagged proteins. After incubating for 5 min, the magnetic beads were separated from the input and washed three times in binding buffer. The pulled down proteins were eluted in binding buffer with 300 mM imidazole and analyzed by SDS-PAGE. A similar method was utilized to examine binding between His-tagged B2′B3 and GST-tagged GTD. Densitometry analysis of Coomassie-stained bands was carried out on digitized images using ImageJ version 1.37 software (Wayne Rasband, National Institutes of Health).

Differential Scanning Fluorimetry—The thermal stability (T_m) of purified $B2'B3_{012}$ and $B2'B3_{027}$ was determined by combining these proteins with SYPRO Orange and performing protein melt reactions. SYPRO Orange increases fluorescence emission by binding to hydrophobic regions of proteins that become exposed during temperature-induced unfolding. In these experiments, an Applied Biosystems 7500 real-time PCR system was used to monitor fluorescence emission of the protein/dye mixture as temperature was stepped from 25 to 99 °C. These reactions were performed in quadruplicate with 0.5 mg/ml protein in a buffer consisting of 20 mM sodium phosphate (pH 7.2) and 137 mM NaCl. The T_m was determined by plotting the first derivative of fluorescence *versus* temperature and then locating the temperature at the midpoint of the transition from folded to unfolded.

RESULTS

The Carboxyl-terminal (B2′B3) Region of $TcdB_{027}$ Forms Higher Order Complexes—Fig. 1*A* shows an overview of the primary structure and domain organization of TcdB. A nomenclature consistent with its characteristics as a single polypeptide A-B toxin was adopted in this study. The GTD is labeled as the A domain, and the remainder of the protein is labeled as subdomains of the B fragment, which constitute the putative cell-binding, autoprocessing, and pore-forming domains of the toxin. The overall sequence identity between $TcdB_{027}$ and $TcdB_{012}$ is 92% (22); however, the level of identity among the different domains of the toxin ranges from 88 to 96%, with the least amount of consensus sequence found in the carboxyl-terminal portion (B2′B3) (Fig. 1*A*). The B2′ region shows 77% identity, and shorter regions reveal patches of sequence in the B2′ region with little or no identity. For example, the 1773–1810 region exhibits 17 residue differences (55% identity), including a smaller (residues 1791–1798) region with 6 of 7 residues that differ between the two forms of the toxin (Fig. 1*C*). Our previous work found that the B2′B3 region of $TcdB_{027}$ does not generate neutralizing antibodies against either form of the toxin, although the same region of $TcdB_{012}$ does induce protection against $TcdB_{012}$ but not against $TcdB_{027}$ (20). In the same study, solid phase ELISA analysis using synthetic peptides found distinct differences in reactive epitopes between the two forms of TcdB. Interestingly, the sequences of many of these epitopes were identical or nearly identical in the two forms of TcdB yet were only reactive in one form of the toxin and not the other. Because of this, we hypothesized that the B2′B3 region of TcdB existed in distinct conformational states that led to significant differences in the exposed epitopes.

In the initial set of experiments, biochemical differences between $B2'B3_{012}$ and $B2'B3_{027}$ were examined. First, the thermal stability of the $B2'B3_{012}$ and $B2'B3_{027}$ was measured using differential scanning fluorimetry. These experiments revealed that $B2'B3_{012}$ had a T_m value of 49.9 °C, whereas $B2'B3_{027}$ had a T_m value of 44.3 °C (Fig. 1*B*). These differences in the T_m values suggested that the two forms of B2′B3 have distinct biochemical properties. These biochemical properties were further explored using both cross-linking and gel filtration approaches. As shown in Fig. 2, the B2′B3 domains of $TcdB_{027}$ and $TcdB_{012}$ were treated with the cross-linker BS^3, and the reaction was examined by SDS-PAGE (Fig. 2*A*) or SDS-agarose gel electrophoresis (AGE) (Fig. 2*B*). As shown by SDS-PAGE analysis, the B2′B3 fragments formed higher order complexes in the presence, but not in the absence, of the cross-linker (Fig. 2*A*). A comparison of $B2'B3_{027}$ and $B2'B3_{012}$ revealed that the multimers formed by $B2'B3_{027}$ were more extensive than those formed by $B2'B3_{012}$ (Fig. 2*A*). Cross-linked $B2'B3_{012}$ formed bands that migrated as dimers, tetramers, and other multimers, whereas the majority of cross-linked $B2'B3_{027}$ was too large to enter the gel (Fig. 2*A*). Because cross-linked $B2'B3_{027}$ formed a large complex that could not be resolved by SDS-PAGE, SDS-

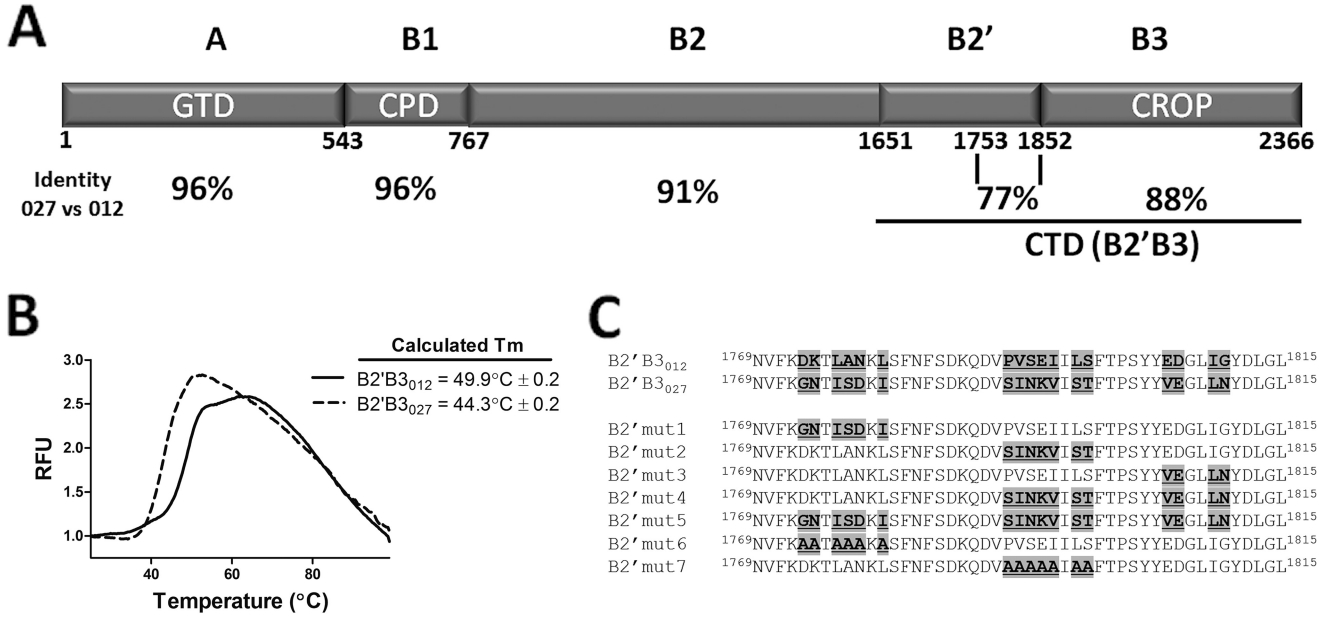

FIGURE 1. **Description of regions of TcdB and thermal stability of the carboxyl terminus (B2′B3) of $TcdB_{012}$ and $TcdB_{027}$.** *A*, domain layout of TcdB and a comparison of sequence identity of TcdB from ribotypes 012 and 027. This depiction demonstrates that the carboxyl terminus of TcdB is the location of much of the sequence variability between $TcdB_{012}$ and $TcdB_{027}$. This figure also reveals a large amount of sequence variability within a 99-amino acid span of the B2′ region, which is the focus on the current studies. *B*, differential scanning fluorimetry was used to determine the thermal stability (T_m) of $B2'B3_{012}$ and $B2'B3_{027}$. The graph depicts increases in relative fluorescence units (*RFU*) as SYPRO Orange binds to hydrophobic regions of proteins that undergo temperature-induced unfolding. These data from the graph were used to calculate the T_m. In the *inset*, the T_m is displayed as the mean and S.D. of four replicates. *C*, sequence alignment comparing a highly variable region of $TcdB_{012}$ and $TcdB_{027}$. This portion of TcdB is the region where the following series of experiments focus and the region targeted for mutagenesis in these studies. The mutants used in these current studies are detailed.

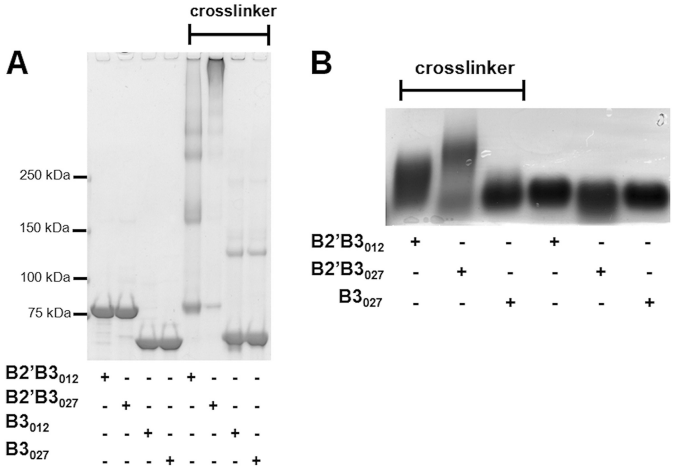

FIGURE 2. **Examination of multimer formation by cross-linking different forms of the carboxyl terminus of TcdB.** Cross-linking of B2′B3 and B3 was performed with BS^3 as described under "Experimental Procedures." The cross-linked protein was resolved by 3–8% gradient SDS-PAGE (*A*) or 1.5% SDS-AGE (*B*) and then stained with Coomassie Blue.

AGE was used to evaluate the cross-linked form of $B2'B3_{027}$. As shown by SDS-AGE, cross-linked $B2'B3_{027}$ migrated more slowly through this gel than cross-linked $B2'B3_{012}$ (Fig. 2*B*). The same cross-linking procedure was applied to the B3 domain to determine whether the B2′ region was necessary for multimer formation. Results from this experiment revealed that the isolated B3 regions did not form substantial higher order complexes in the presence of cross-linker (Fig. 2). These data suggest that $B2'B3_{027}$ could exist in a substantially higher order complex than $B2'B3_{012}$ because of sequence differences in the B2′ region.

To examine multimer formation more closely, the next set of experiments used gel filtration (GF) to follow multimer formation in solution and examine the effects of mutating candidate residues in the B2′ region of $B2'B3_{012}$. In line with the cross-linking data, neither B3 domain formed a higher order complex (Fig. 3, *A* and *B*), and only a small amount of $B2'B3_{012}$ was able to multimerize (Fig. 3*C*). However, GF analysis revealed that all of the $B2'B3_{027}$ eluted in the void volume (Fig. 3*D*), which is indicative of a high order complex larger than 600 kDa. Experiments were next performed to determine whether specific $B2'_{027}$ residues involved in multimerization could be identified. To accomplish this, select mutants (summarized in Fig. 1*C*) were generated wherein residues in $B2'B3_{012}$ were replaced with the corresponding sequence from $B2'_{027}$ (Fig. 3, *E–H*). Although none of the mutants exhibited a GF profile identical to that of $B2'B3_{027}$, GF analysis revealed that three of the four mutants (B2′mut1, B2′mut2, and B2′mut5) had either minor or major peaks indicative of complexes larger than observed with $B2'B3_{012}$. Additionally, these mutants were analyzed by BS^3 cross-linking, and increased multimerization was also observed in B2′mut1, B2′mut2, and B2′mut5 (Fig. 3*J*). Finally, candidate residues in $B2'B3_{027}$ were mutated to alanines (Fig. 1*C*) and examined to determine whether this decreased multimer formation. As shown by GF, alanine substitutions at the target residues in $B2'B3_{027}$ reduced the ability of $B2'B3_{027}$ to form multimers (Fig. 3*I*). Collectively, these data suggest that amino acids 1773–1780 (B2′mut1 and B2′mut6) and 1791–1798 (B2′mut2) help support multimerization in $B2'B3_{027}$.

Identification of Regions That Influence Exposure of Neutralizing Epitopes—The data shown in Figs. 2 and 3 indicate that purified $B2'B3_{027}$ exists in a higher order complex that is

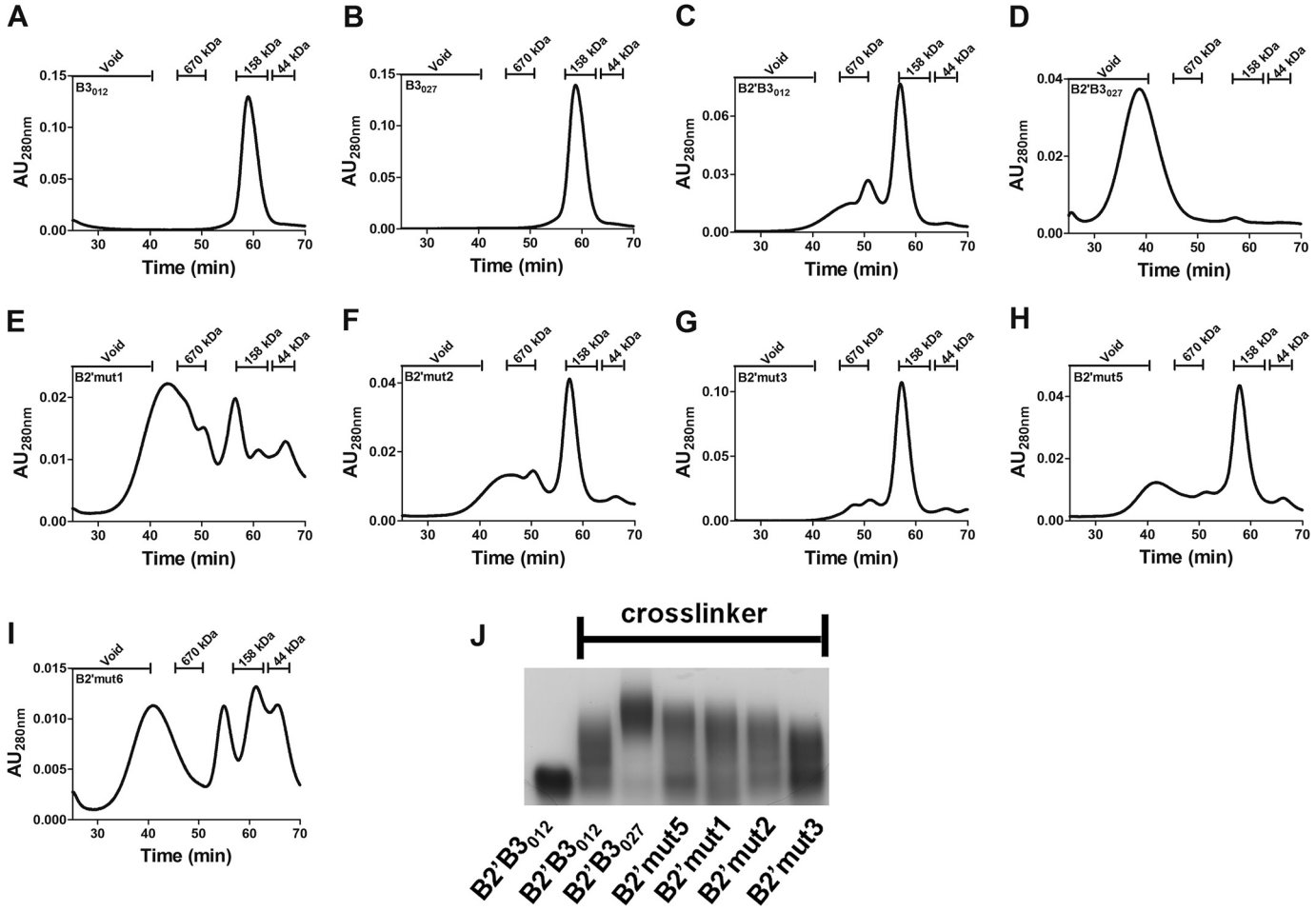

FIGURE 3. **Multimer analysis by gel filtration and cross-linking.** *A–I*, multimer formation of B2′B3 or B3 was evaluated by gel filtration. In these profiles, multimer formation was determined by measuring the elution times (min) of these proteins from a Superose 6 10/300 GL column. Protein elution was monitored by measuring absorbance at 280 nm (absorbance units at 280 nm ($AU_{280\ nm}$)). The retention times of the standards are shown at the *top* of each *panel*. *J*, BS^3 cross-linking was performed as described under "Experimental Procedures," and 1.5% SDS-AGE was used to separate cross-linked proteins. The mutant forms are described in the legend to Fig. 1*C*.

dependent on a set of residues in the B2′ region. We next asked whether these differences in complex formation might impact the exposure of neutralizing epitopes. To identify regions targeted by neutralizing antibodies, we utilized an assay (Fig. 4) in which B2′B3 fragments were assessed for their ability to block neutralizing antiserum. Specifically, polyclonal rabbit serum raised against $B2'B3_{012}$ ($\alpha B2'B3_{012}$), which we had previously reported to neutralize $TcdB_{012}$, was incubated with the entire $B2'B3_{012}$ region (residues 1652–2366) or the B3 region (residues 1853–2366) to adsorb antibodies. $B2'B3_{012}$ but not $B3_{012}$ blocked the neutralizing antiserum (Fig. 4*A*). The region of TcdB important for neutralization with this antiserum was further narrowed down when a purified segment of B2′ (residues 1753–1852) was found to block toxin neutralization (Fig. 4*A*). Next, the B2′B3 region of $TcdB_{027}$ was examined and found to be less effective at blocking neutralizing antibodies than $B2'B3_{012}$ (Fig. 4*A*), which corresponds to our previous findings that indicate that $B2'B3_{027}$ does not generate a strong antibody-mediated neutralizing response like $B2'B3_{012}$ (20).

Sequence Variation within B2′ Alters Exposure of Neutralizing Epitopes—Experiments next examined various B2′B3 mutants to determine whether sequences in the B2′ region influence neutralizing epitopes. As shown in Fig. 4*B*, when residues from $TcdB_{027}$ were substituted in the 1791–1798 (B2′mut2) and 1805–1810 (B2′mut3) regions of $B2'B3_{012}$, there was no detectable impact on the ability of this fragment to block neutralizing antibodies. In contrast, $B2'B3_{012}$ lost the ability to block neutralizing antibodies when $TcdB_{027}$ residues were substituted into the 1773–1780 (B2′mut1) region. In line with this, a double mutant (B2′mut4) possessing mutations at 1791–1798 and 1805–1810 was able to block neutralizing antibodies, whereas a triple mutant (B2′mut5) containing mutations in all three regions was unable to block neutralizing antibodies. These data suggest that the 1773–1780 region encodes and/or influences the exposure of neutralizing epitopes in the B2′B3 region of $TcdB_{012}$.

In our next experiment, we determined whether the linear epitope corresponding to residues 1773–1780 of $TcdB_{012}$ could bind neutralizing antibodies. Therefore, we designed a small peptide that contained residues 1773–1780 of $TcdB_{012}$ and determined whether this peptide could absorb neutralizing antibodies. As shown in Fig. 4*C*, we could not detect any loss of activity of the antibody. This result suggested that the 1773–1880 region may be influencing the exposure of neutralizing

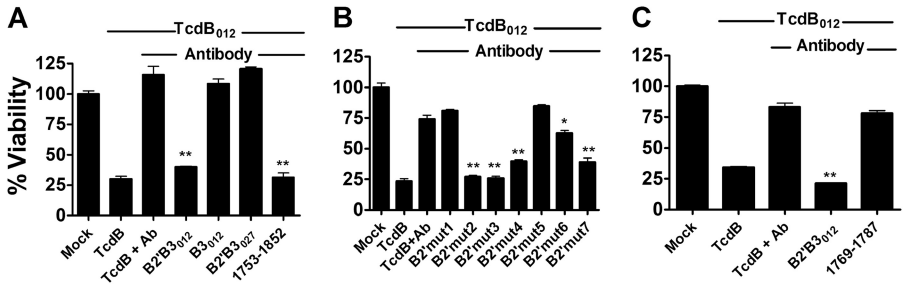

FIGURE 4. **Neutralizing antibodies are absorbed by different forms of the B2′B3.** *A–C*, bar graphs represent the percentage of viable CHO cells after treatment for 24 h with 3.8 pM purified native $TcdB_{012}$. Cell viability was measured by a colorimetric reaction using WST-8 dye. To neutralize $TcdB_{012}$, the toxin was preincubated for 30 min with a 1:100 dilution of antiserum against $B2'B3_{012}$ ($\alpha B2'B3_{012}$). The neutralization activities of the antiserum were absorbed by incubating the antiserum with B2′B3 for 30 min before the addition of purified native $TcdB_{012}$. *A*, this assay used 60 nM of $B2'B3_{012}$, $B3_{012}$, or $B2'B3_{027}$. The fragment of $TcdB_{012}$ from amino acid 1751 to 1853 was used at a concentration of 10 μM. *B*, 48 nM mutated B2′B3 (described in the legend to Fig. 1) was used in these experiments. *C*, this experiment was performed with 30 nM $B2'B3_{012}$ or 45 μM peptide spanning residues 1769–1787 of $TcdB_{012}$. Data are presented as mean ($n = 3$) ± S.D. (*error bars*). *Asterisks* indicate that antibody neutralization is significantly reduced. *, $p < 0.05$; **, $p < 0.005$.

epitopes in $B2'B3_{027}$, perhaps by increasing multimerization, as observed in Fig. 3. To test this possibility, we examined the B2′mut6 and B2′mut7 mutants that contained alanine substitutions at the putative critical residues in $B2'B3_{027}$. Strikingly, both mutants, containing a string of alanine substitutions, gained the capacity to block neutralizing antiserum (Fig. 4*B*). These results suggested that the $B2'B3_{027}$ region encodes neutralizing epitopes, but these are structurally occluded by sequences in the B2′ subdomain.

Antibody-mediated Neutralization of TcdB Hybrids—The data described above indicated that sequence differences in the B2′ region of $B2'B3_{012}$ and $B2'B3_{027}$ impacted the exposure of neutralizing epitopes. In the next experiment, we confirmed that observation in the context of the holotoxin and determined whether other regions of TcdB outside of B2′B3 might also influence the exposure of neutralizing epitopes. For these experiments, DNA segments encoding B2′B3 in the two forms of TcdB were swapped to generate hybrids of $TcdB_{027}$ and $TcdB_{012}$ with the reciprocal B2′B3 domains ($TcdB_{027}$/$B2'B3_{012}$ and $TcdB_{012}$/$B2'B3_{027}$). In initial experiments, all four forms of the toxins had statistically identical viability curves when toxin activity was examined in the presence of serum from unvaccinated rabbits (Fig. 5*A*). These toxins were then tested for their sensitivity to antibodies raised against the $B2'B3_{012}$ ($\alpha B2'B3_{012}$). As shown in Fig. 5*B*, $\alpha B2'B3_{012}$ was able to neutralize $TcdB_{012}$, whereas $TcdB_{027}$ was less susceptible to neutralization by this antiserum, which was observed previously (20). Examination of the two hybrid toxins revealed that $TcdB_{027}$/$B2'B3_{012}$ was more sensitive to neutralization by $\alpha B2'B3_{012}$ than $TcdB_{012}$/$B2'B3_{027}$ (Fig. 5*B*). Unexpectedly, $TcdB_{027}$/$B2'B3_{012}$ was found to be more sensitive to neutralization by $\alpha B2'B3_{012}$ than $TcdB_{012}$ (Fig. 5*B*). This unexpected observation was confirmed when $TcdB_{027}$/$B2'B3_{012}$ was also found to be more sensitive than $TcdB_{012}$ to neutralization with antibodies against $B2'B3_{027}$ (data not shown). These data suggest the amino-terminal region of the toxin could be influencing the exposure of epitopes in the B2′B3 domain.

The B2′ Region Facilitates Binding between $B2'B3_{027}$ and Full-length TcdB—The results above suggest that protein-protein interactions between domains of TcdB may be influencing the overall folding and exposure of neutralizing epitopes. Based on the multimerization data, we hypothesized that the B2′

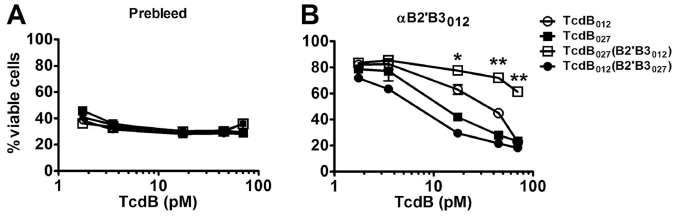

FIGURE 5. **Antiserum neutralization of toxin after B2′B3 domains of $TcdB_{012}$ and $TcdB_{027}$ are exchanged.** The graphs represent the percentage of viable CHO cells after treatment for 24 h with different forms of TcdB. Measurement of cell viability was accomplished by a colorimetric reaction using WST-8 dye. TcdB neutralization was performed by preincubating the toxin for 30 min with a 1:100 dilution of prebleed serum or antiserum against $B2'B3_{012}$ ($\alpha B2'B3_{012}$). Data are presented as mean ($n = 3$) ± S.D. (*error bars*). *Asterisks* indicate significant differences between $TcdB_{012}$ and $TcdB_{027}$/$B2'B3_{012}$. *, $p < 0.05$; **, $p < 0.005$.

region of TcdB may serve as an important site for mediating protein-protein contacts between domains of TcdB. To test this possibility, we first determined whether we could detect binding between B2′B3 and the holotoxin. Therefore, we performed pull-down experiments using $B2'B3_{027}$ or $B2'B3_{012}$ immobilized to cobalt-coated magnetic beads via their His tags. In these experiments, the B2′B3 fragment was mixed with $TcdB_{027}$ or $TcdB_{012}$, and the pellets from the pull-down were then examined by SDS-PAGE. As shown in Fig. 6*A*, when the pull-down was performed using $B2'B3_{027}$ as the bait, both $TcdB_{027}$ and $TcdB_{012}$ were detected on the gel. In contrast, using $B2'B3_{012}$ as the bait did not result in the pull-down of either form of the holotoxin (Fig. 6*A*). When the $B3_{027}$ domain alone was used in the pull-down, full-length TcdB could not be detected on the gel (Fig. 6*B*), which indicates that the B2′ region is necessary for protein-protein interactions between $B2'B3_{027}$ and full-length toxin. The residues in B2′ capable of interacting with full-length TcdB were narrowed down using the mutants described in Fig. 1*C*. As shown in Fig. 6, *C* and *D*, $B2'B3_{012}$ gained the ability to bind TcdB when amino acids 1773–1780 (B2′mut1) or 1791–1798 (B2′mut2) were replaced with the corresponding sequence from $B2'B3_{027}$. In contrast, $B2'B3_{012}$ did not gain the ability to bind TcdB when amino acids 1805–1810 were changed to the $B2'B3_{027}$ sequence. These data demonstrate that the B2′ region of the $B2'B3_{027}$ is important for binding to full-length TcdB and suggest that B2′ might be involved in mediating interdomain contacts.

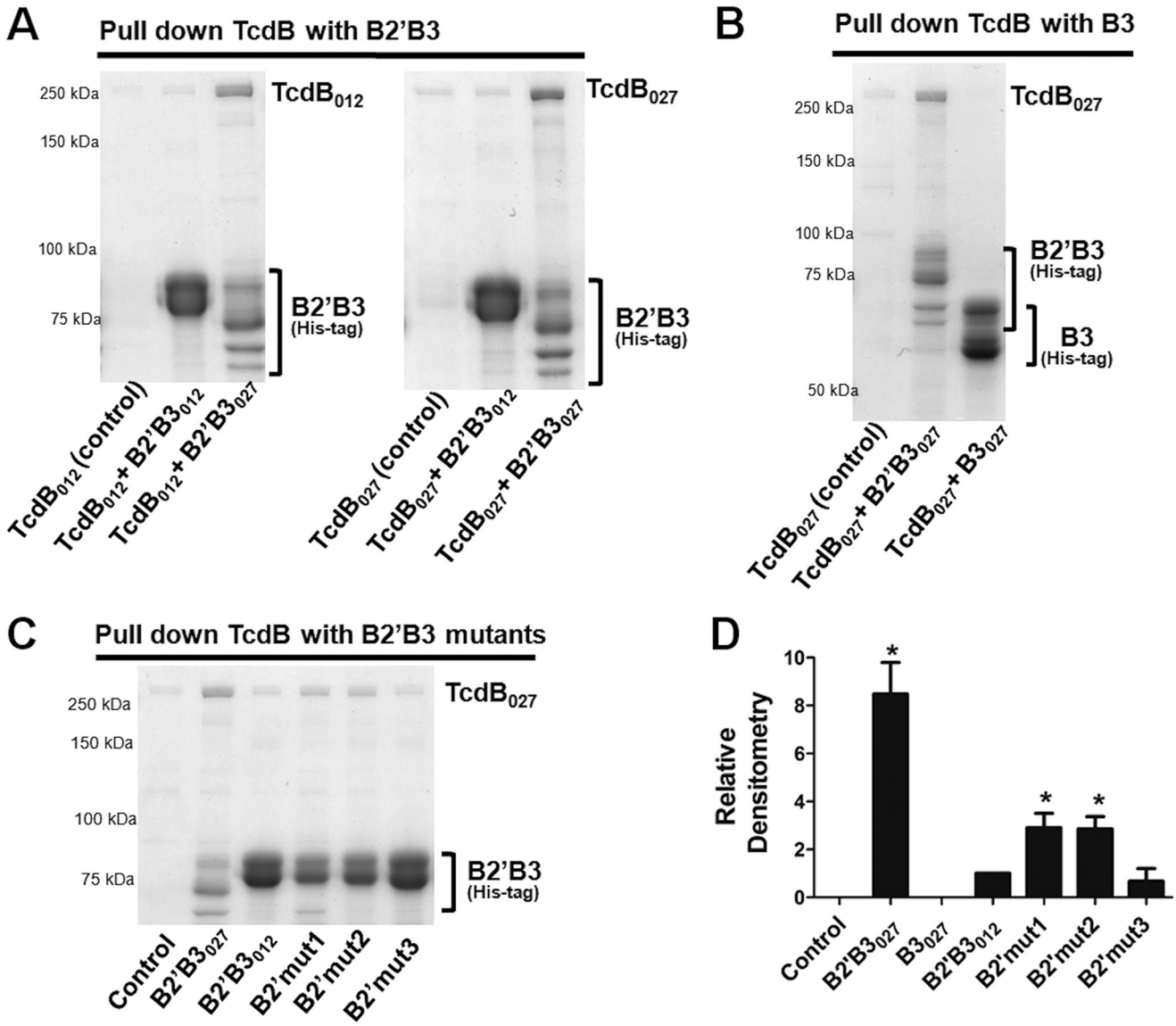

FIGURE 6. **Analysis of interactions between full-length TcdB and the B2′B3 domain.** Pull-down experiments were utilized to examine binding between full-length TcdB and B2′B3. These experiments were carried out with TcdB purified from *C. difficile* and recombinant His-tagged B2′B3 purified from *E. coli*. Incubations were done for 1 h at 37 °C with 450 nM TcdB and 2 μM B2′B3. His-tagged B2′B3 was pulled down with cobalt-coated magnetic beads, and binding between B2′B3 and TcdB was visualized by SDS-PAGE and Coomassie staining. *A*, SDS-PAGE demonstrating binding between B2′B3 and TcdB from different ribotypes. *B*, SDS-PAGE depicting lack of binding between $B3_{027}$ and $TcdB_{027}$. *C*, SDS-PAGE examining binding between $TcdB_{027}$ and mutant forms of B2′B3 described in the legend to Fig. 1*C*. *D*, the bar graph represents the densitometry analysis of three Coomassie-stained gels from the data in *A*–*C*. Results are presented as mean ($n = 3$) ± S.D. (*error bars*). *Asterisks* indicate significance when compared with $B2'B3_{012}$. *, $p < 0.01$.

Because the amino-terminal region of TcdB appears to influence the exposure of epitopes in the B2′B3 region (Fig. 5), we hypothesized that protein-protein interactions between the B2′B3 region and the holotoxin could be impacted by alterations to the amino-terminal region. To begin to explore the influence of the amino terminus on binding between B2′B3 and the toxin, we first determined whether $B2'B3_{027}$ could bind the GTD, which corresponds to amino acids 1–543 of TcdB (Fig. 1A). As shown by the pull-down experiments in Fig. 7, *A*–*C*, $B2'B3_{027}$ was not able to bind either GTD_{012} or GTD_{027}. As another method for investigating the influence of the amino terminus on binding between the B2′B3 region and the toxin, we took advantage of the autoprocessing characteristic of TcdB. Upon induction of autoprocessing, the CPD cleaves TcdB between residues 543 and 544, thus separating the GTD (residues 1–543) from the remainder of the toxin (residues 544–2366). Therefore, if the amino-terminal region modulates interactions between B2′B3 and the holotoxin, differences should be detected in the level of $B2'B3_{027}$ binding to the processed and unprocessed forms of the toxin. Hence, we carried out *in vitro* autoprocessing under conditions that yielded a mixture of uncleaved and cleaved toxin, with a majority of the toxin remaining in the uncleaved form (Fig. 7*D*). A pull-down was then performed between $B2'B3_{027}$ and partially processed TcdB. As shown in Fig. 7*D*, $B2'B3_{027}$ preferentially pulled down processed TcdB (residues 544–2366) rather than unprocessed TcdB (residues 1–2366) (Fig. 7*D*). A similar result was observed for both $TcdB_{012}$ and $TcdB_{027}$. These results indicate that $B2'B3_{027}$ binds a region located between 544 and 2366 and suggest

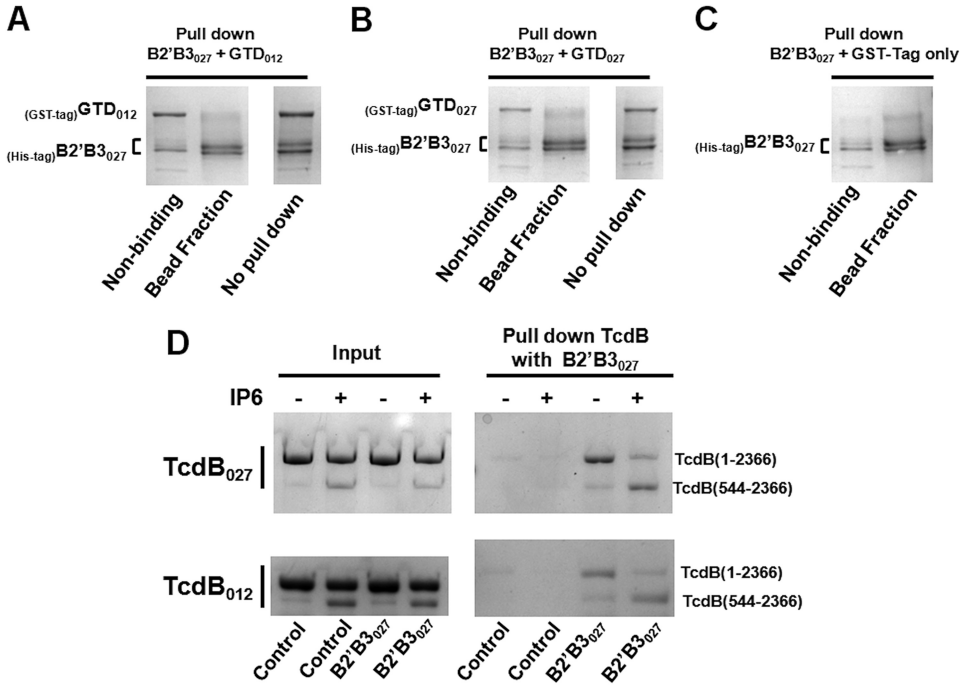

FIGURE 7. **Binding between full-length TcdB and B2′B3$_{027}$ is influenced by the amino terminus of TcdB.** *A–C*, pull-down experiments were used to examine binding between GTD and B2′B3. These experiments were carried out with purified His-tagged B2′B3 and purified GST-tagged GTD. Incubations of 450 nM GTD with 2 μM B2′B3 were performed for 1 h at 37 °C. His-tagged B2′B3 was pulled down with cobalt-coated magnetic beads, and interactions between B2′B3 and GTD were assessed using SDS-PAGE and Coomassie staining. *D*, IP6 processing was used to separate the amino terminus from TcdB and determine whether removal of the amino terminus influences binding between TcdB and B2′B3$_{027}$. To activate TcdB processing, 450 nM TcdB was incubated with 100 μM IP6 for 1 h at 37 °C. This was followed by the addition of 2 μM B2′B3$_{027}$ and another incubation for 1 h at 37 °C. His-tagged B2′B3$_{027}$ was pulled down with cobalt-coated magnetic beads, and binding between B2′B3$_{027}$ and TcdB was visualized by SDS-PAGE and Coomassie staining. The gel labeled *Input* illustrates the ratio of processed to unprocessed TcdB that does not pull down with B2′B3$_{027}$. The gel labeled *Pull down* shows the ratio of processed to unprocessed TcdB that binds B2′B3$_{027}$.

that the GTD (residues 1–543) is obstructing the site on TcdB that B2′B3$_{027}$ binds.

DISCUSSION

The emergence of new strains of *C. difficile* presents an ongoing challenge to clinicians. Strains such as the 027 ribotype have predominated in several geographical regions during the past decade and correlate with increases in the mortality rate of CDI (24–26). Not only does this change in *C. difficile* epidemiology complicate treatment, but patients are more likely to relapse if infected by the 027 ribotype (27). Furthermore, our previous work has shown that antibodies capable of neutralizing TcdB from historical strains do not equally neutralize TcdB from 027 strains (20). As part of the previous study, we also mapped reactive epitopes in the B2′B3 regions of the two forms of TcdB. Curiously, despite sharing common sequences, antibodies recognizing epitopes in B2′B3$_{012}$ did not react with the identical sequences in B2′B3$_{027}$. This led us to speculate that both sequence variations and conformational differences influenced antibody reactivity and altered sensitivity to neutralization. In the current study, we sought to identify key sequence differences in TcdB$_{027}$ and TcdB$_{012}$ that account for variations in neutralization by antibodies against TcdB. The data indicate that sequence differences may not only alter specific neutralizing epitopes but also confer structural variations that cloak epitopes that would otherwise be subject to antibody targeting.

The experiments in this study focused on the carboxyl-terminal region of TcdB with a particular emphasis on the B2′ sequence. This region is of particular interest because recent work by Zhang *et al.* (28) showed that the 1756–1852 region was required for TcdB toxicity. Moreover, a comparison of the B2′ regions showed only 77% identity between the two forms of TcdB, which is notably less than the 92% identity found across the full length of the two toxins. Thus, given the sequence differences between the two forms of the toxin and the demonstrated importance of this region in intoxication, we reasoned that this portion of the toxin could encode critical neutralizing epitopes that differed between TcdB$_{027}$ and TcdB$_{012}$. In Fig. 4, an antibody-blocking assay was used to map critical neutralization regions to the B2′ and pinpoint sequence variations in the B2′ that alter neutralizing epitopes. Interestingly, results from the antibody blocking assay indicated that both B2′B3$_{012}$ and B2′B3$_{027}$ have neutralizing epitopes, but B2′B3$_{027}$ exists in a conformation that cloaks these epitopes. To explain the mechanism of epitope cloaking, biochemical analyses of the B2′B3 regions were conducted that revealed that these regions exist in a multimeric state. Using a chemical cross-linking approach as well as GF analysis, we found that the B2′ region was necessary for the multimerization of B2′B3 because this activity was not observed when only the B3 fragment was examined (Figs. 2 and 3). These data also indicated that B2′B3$_{027}$ multimerized more readily than B2′B3$_{012}$, and increased multimerization could be conferred to B2′B3$_{012}$ by substituting amino acids encoded by the 027 form of the toxin, which correlates with the antibody-blocking assay.

The ability of the B2′B3 region to multimerize provides important clues about the function of this toxin and the mechanism of epitope cloaking. The multimerization of the B2′B3 suggests that full-length toxin may form multimers, but data from our group suggest that the full-length toxin exists as a monomer at neutral pH (data not shown). However, this does not exclude the possibility that TcdB may form multimers under certain buffer conditions that the toxin encounters during the cellular entry process. Another interpretation of the multimerization data suggests that B2′B3 multimerization may be related to intramolecular interactions that exist within monomeric TcdB. Thus, the multimerization assay may be detecting an intramolecular interaction that appears as multimerization when the analysis is performed on the B2′B3 fragment alone. This latter possibility is supported by experimental data in Figs. 5 and 6.

In Fig. 6, we determined whether the molecular contacts that confer multimerization had functionality in the full-length toxin. In these pull-down experiments, we demonstrated that the $B2'B3_{027}$ fragment could bind full-length toxin, whereas $B2'B3_{012}$ could not. As with the multimerization data, the B2′ region was essential for this activity, and binding between $B2'B3_{012}$ and TcdB could be conferred to $B2'B3_{012}$ by substituting amino acids encoded by the 027 form of the toxin. Next, we further explored the idea of intramolecular interactions cloaking neutralizing epitopes within the full-length toxin. In Fig. 5, the B2′B3 regions of $TcdB_{012}$ and $TcdB_{027}$ were swapped, yielding TcdB hybrids ($TcdB_{012}$/$B2'B3_{027}$ and $TcdB_{027}$/$B2'B3_{012}$). These experiments suggested that the amino-terminal portion of the toxin influences the exposure of neutralizing epitopes. For instance, when $B2'B3_{012}$ is combined with the amino terminus of $TcdB_{027}$, the B2′B3 domain appears to become more accessible to the neutralizing antibody (Fig. 5*B*). This suggests that the amino-terminal region interacts with the carboxyl-terminal portion of the toxin, thereby changing the exposure of neutralizing epitopes. This possibility was further examined by taking advantage of the autoprocessing activity of TcdB. Following autoprocessing, which dissociates residues 1–543 from the 544–2366 region, $B2'B3_{027}$ was found to bind the larger processed fragment (residues 544–2366) better than the intact holotoxin (residues 1–2366) (Fig. 7*D*). This observation suggests that the amino terminus of TcdB is obscuring regions that can bind the B2′B3 region, thus supporting the idea that the amino-terminal region of TcdB is influencing the accessibility of neutralizing epitopes in the B2′B3 region of TcdB. Interestingly, the cryo-EM structure of TcdB suggests contacts between the GTD and a region proximal to the B3 domain of TcdB, and this contact is lost following autoprocessing (29). Further studies that map these contact regions may provide important information on how these two distal portions of the toxin interact.

The extent to which the variations in TcdB will influence interactions with antibodies has not been explored in detail and could have important consequences as disease-causing strains of *C. difficile* continue to emerge. In addition to ribotype 027, ribotype 078 has recently surfaced as a highly virulent strain in humans. Examining the sequence of TcdB from ribotype 078, we discovered that the B2′ region more closely resembles the 012 ribotype (98% identity) than the 027 ribotype (78% identity). When we inspect residues that were identified in this study as critical, we find that residues 1773–1780 from $TcdB_{078}$ exactly match $TcdB_{012}$. However, examination of residues 1791–1798 shows that only 6 of the 8 amino acids agree with $TcdB_{012}$. Interestingly, one of the residues in this region of $TcdB_{078}$ matches $TcdB_{027}$ (Ser-1797), and one of the residues is unique to $TcdB_{078}$ (Ala-1798). This unique residue is a serine in $TcdB_{012}$ and a threonine in $TcdB_{027}$. These subtle sequence changes in $TcdB_{078}$ could impact the structure of TcdB as well as interactions with antibodies. Additionally, these changes could provide clues to the future of emergent stains of *C. difficile.*

These variations in TcdB could also influence vaccination and therapeutic antibody efficacy. A study by Marozsan *et al.* (30) found that the humanized monoclonal antibodies CDA1 and CDB1, targeting TcdA and TcdB, were substantially less effective against toxin from the 027 ribotype compared with other ribotypes, such as the 012 ribotype. CDB1 is also referred to as bezlotoxumab, which is a TcdB-specific humanized monoclonal antibody currently in phase 3 clinical trials (31). Recently, Orth *et al.* (32) determined the crystal structure of bezlotoxumab bound to epitopes in the carboxyl-terminal region of TcdB. The sequence of the target antigen for the crystallization studies was derived from $TcdB_{012}$, and using a combination of approaches, the authors identified regions of the toxin that were blocked by bezlotoxumab. Within the regions found to be blocked by bezlotoxumab, we noted that only two residues (Asn-1912 and Glu-2033) differed between $TcdB_{027}$ and $TcdB_{012}$. In $TcdB_{027}$, Asn-1912 is replaced with aspartic acid, and Glu-2033 is replaced with an alanine. Both of these changes could impact charge interactions, but they do not seem to be dramatic in the context of the entire sequence. Moreover, of the 22 TcdB residues situated within 4.0 Å of contact with the antibody complementarity-determining region, only four differed between the two forms of the toxin. Of those residues, none appear to show intimate interactions with residues in the complementarity-determining region. Based on this assessment, we can reasonably conclude that bezlotoxumab should interact with target epitopes both in $TcdB_{027}$ and $TcdB_{012}$, yet the neutralization experiments suggest that $TcdB_{027}$ is less sensitive to the antibody (30). More recently, Hernandez *et al.* (33) performed a comprehensive analysis of bezlotoxumab reactivity with TcdB from several ribotypes and found that subtle sequence variations do indeed affect the EC_{50}, but this can be overcome by reasonable increases in the amounts of antibody applied to the toxin. The extent to which intramolecular or intermolecular interactions shield these and other specific neutralizing epitopes has yet to be determined.

Identifying the sequence of epitopes cloaked by the 1752–1851 region is the subject of ongoing studies in our laboratory; however, evidence in the literature supports the idea that candidate epitopes reside between residues 1853 and 2066. Leuzzi *et al.* (34) found that a TcdB fragment covering the 1853–2366 region of the toxin generated a protective antibody response, whereas smaller fragments (2056–2366 and 2157–2366) did not induce a protective response, despite stimulating high antibody titers. This suggests that the 1853–2056 region could con-

tain neutralizing epitopes, which correlates with the effectiveness of bezlotoxumab mentioned above. In a previous study, we mapped reactive epitopes in B2′B3 for both forms of the toxin (20). $TcdB_{012}$ has four unique epitopes, and $TcdB_{027}$ has only one unique epitope in this region. Moreover, the toxins appear to share at least five common epitopes in this region of the protein. It will be of great interest to determine whether the two forms of TcdB share critical neutralizing epitopes, which are more effectively blocked in $TcdB_{027}$.

A high resolution three-dimensional structure has not been reported for either $TcdB_{012}$ or $TcdB_{027}$, making it difficult to know the precise structural differences between the two forms of the toxin. Moreover, the crystal structure itself might not reveal intermolecular interactions that influence exposure of epitopes in the B2′B3 region of the toxin. However, the findings that structural differences influence exposure of epitopes with shared sequences are bolstered by two earlier studies from our group. Previously, we found that $TcdB_{027}$ underwent acid-induced conformational changes at a higher pH than $TcdB_{012}$ (22). In a second study analyzing the autoproteolytic activity of TcdB, we found that the CPD of $TcdB_{012}$ was more sensitive to labeling with an exogenous probe than the CPD from $TcdB_{027}$ (21). Taken together, these data consistently support the idea that $TcdB_{027}$ and $TcdB_{012}$ exist in distinct conformations that affect their biochemical activities and antigenicity.

REFERENCES

1. Voth, D. E., and Ballard, J. D. (2005) *Clostridium difficile* toxins: mechanism of action and role in disease. *Clin. Microbiol. Rev.* **18,** 247–263
2. Rupnik, M., Braun, V., Soehn, F., Janc, M., Hofstetter, M., Laufenberg-Feldmann, R., and von Eichel-Streiber, C. (1997) Characterization of polymorphisms in the toxin A and B genes of *Clostridium difficile*. *FEMS Microbiol. Lett.* **148,** 197–202
3. Rupnik, M., Avesani, V., Janc, M., von Eichel-Streiber, C., and Delmée, M. (1998) A novel toxinotyping scheme and correlation of toxinotypes with serogroups of *Clostridium difficile* isolates. *J. Clin. Microbiol.* **36,** 2240–2247
4. Lyras, D., O'Connor, J. R., Howarth, P. M., Sambol, S. P., Carter, G. P., Phumoonna, T., Poon, R., Adams, V., Vedantam, G., Johnson, S., Gerding, D. N., and Rood, J. I. (2009) Toxin B is essential for virulence of *Clostridium difficile*. *Nature* **458,** 1176–1179
5. Savidge, T. C., Pan, W. H., Newman, P., O'brien, M., Anton, P. M., and Pothoulakis, C. (2003) *Clostridium difficile* toxin B is an inflammatory enterotoxin in human intestine. *Gastroenterology* **125,** 413–420
6. Sun, X., Savidge, T., and Feng, H. (2010) The enterotoxicity of *Clostridium difficile* toxins. *Toxins* **2,** 1848–1880
7. Genisyuerek, S., Papatheodorou, P., Guttenberg, G., Schubert, R., Benz, R., and Aktories, K. (2011) Structural determinants for membrane insertion, pore formation and translocation of *Clostridium difficile* toxin B. *Mol. Microbiol.* **79,** 1643–1654
8. Pfeifer, G., Schirmer, J., Leemhuis, J., Busch, C., Meyer, D. K., Aktories, K., and Barth, H. (2003) Cellular uptake of *Clostridium difficile* toxin B: translocation of the N-terminal catalytic domain into the cytosol of eukaryotic cells. *J. Biol. Chem.* **278,** 44535–44541
9. Barth, H., Pfeifer, G., Hofmann, F., Maier, E., Benz, R., and Aktories, K. (2001) Low pH-induced formation of ion channels by *Clostridium difficile* toxin B in target cells. *J. Biol. Chem.* **276,** 10670–10676
10. Qa'Dan, M., Spyres, L. M., and Ballard, J. D. (2000) pH-induced conformational changes in *Clostridium difficile* toxin B. *Infect. Immun.* **68,** 2470–2474
11. Zhang, Z., Park, M., Tam, J., Auger, A., Beilhartz, G. L., Lacy, D. B., and Melnyk, R. A. (2014) Translocation domain mutations affecting cellular toxicity identify the *Clostridium difficile* toxin B pore. *Proc. Natl. Acad. Sci. U.S.A.* **111,** 3721–3726
12. Reineke, J., Tenzer, S., Rupnik, M., Koschinski, A., Hasselmayer, O., Schrattenholz, A., Schild, H., and von Eichel-Streiber, C. (2007) Autocatalytic cleavage of *Clostridium difficile* toxin B. *Nature* **446,** 415–419
13. Rupnik, M., Pabst, S., Rupnik, M., von Eichel-Streiber, C., Urlaub, H., and Söling, H. D. (2005) Characterization of the cleavage site and function of resulting cleavage fragments after limited proteolysis of *Clostridium difficile* toxin B (TcdB) by host cells. *Microbiology* **151,** 199–208
14. Li, S., Shi, L., Yang, Z., and Feng, H. (2013) Cytotoxicity of *Clostridium difficile* toxin B does not require cysteine protease-mediated autocleavage and release of the glucosyltransferase domain into the host cell cytosol. *Pathog. Dis.* **67,** 11–18
15. Farrow, M. A., Chumbler, N. M., Lapierre, L. A., Franklin, J. L., Rutherford, S. A., Goldenring, J. R., and Lacy, D. B. (2013) *Clostridium difficile* toxin B-induced necrosis is mediated by the host epithelial cell NADPH oxidase complex. *Proc. Natl. Acad. Sci. U.S.A.* **110,** 18674–18679
16. Chumbler, N. M., Farrow, M. A., Lapierre, L. A., Franklin, J. L., Haslam, D., Goldenring, J. R., and Lacy, D. B. (2012) *Clostridium difficile* Toxin B causes epithelial cell necrosis through an autoprocessing-independent mechanism. *PLoS Pathog.* **8,** e1003072
17. Wohlan, K., Goy, S., Olling, A., Srivaratharajan, S., Tatge, H., Genth, H., and Gerhard, R. (2014) Pyknotic cell death induced by *Clostridium difficile* TcdB: chromatin condensation and nuclear blister are induced independently of the glucosyltransferase activity. *Cell Microbiol.* **16,** 1678–1692
18. Valiente, E., Cairns, M. D., and Wren, B. W. (2014) The *Clostridium difficile* PCR ribotype 027 lineage: a pathogen on the move. *Clin. Microbiol. Infect.* **20,** 396–404
19. Stabler, R. A., He, M., Dawson, L., Martin, M., Valiente, E., Corton, C., Lawley, T. D., Sebaihia, M., Quail, M. A., Rose, G., Gerding, D. N., Gibert, M., Popoff, M. R., Parkhill, J., Dougan, G., and Wren, B. W. (2009) Comparative genome and phenotypic analysis of *Clostridium difficile* 027 strains provides insight into the evolution of a hypervirulent bacterium. *Genome Biol.* **10,** R102
20. Lanis, J. M., Heinlen, L. D., James, J. A., and Ballard, J. D. (2013) *Clostridium difficile* 027/BI/NAP1 encodes a hypertoxic and antigenically variable form of TcdB. *PLoS Pathog.* **9,** e1003523
21. Lanis, J. M., Hightower, L. D., Shen, A., and Ballard, J. D. (2012) TcdB from hypervirulent *Clostridium difficile* exhibits increased efficiency of autoprocessing. *Mol. Microbiol.* **84,** 66–76
22. Lanis, J. M., Barua, S., and Ballard, J. D. (2010) Variations in TcdB activity and the hypervirulence of emerging strains of *Clostridium difficile*. *PLoS Pathog.* **6,** e1001061
23. Yang, G., Zhou, B., Wang, J., He, X., Sun, X., Nie, W., Tzipori, S., and Feng, H. (2008) Expression of recombinant *Clostridium difficile* toxin A and B in *Bacillus megaterium*. *BMC Microbiol.* **8,** 192
24. Wilcox, M. H., Shetty, N., Fawley, W. N., Shemko, M., Coen, P., Birtles, A., Cairns, M., Curran, M. D., Dodgson, K. J., Green, S. M., Hardy, K. J., Hawkey, P. M., Magee, J. G., Sails, A. D., and Wren, M. W. (2012) Changing epidemiology of *Clostridium difficile* infection following the introduction of a national ribotyping-based surveillance scheme in England. *Clin. Infect. Dis.* **55,** 1056–1063
25. Bauer, M. P., Notermans, D. W., van Benthem, B. H., Brazier, J. S., Wilcox, M. H., Rupnik, M., Monnet, D. L., van Dissel, J. T., and Kuijper, E. J. (2011) *Clostridium difficile* infection in Europe: a hospital-based survey. *Lancet* **377,** 63–73
26. Wilcox, M. H., and Freeman, J. (2006) Epidemic *Clostridium difficile*. *N. Engl. J. Med.* **354,** 1199–1203; author reply 1199–1203
27. Marsh, J. W., Arora, R., Schlackman, J. L., Shutt, K. A., Curry, S. R., and Harrison, L. H. (2012) Association of relapse of *Clostridium difficile* disease with BI/NAP1/027. *J. Clin. Microbiol.* **50,** 4078–4082
28. Zhang, Y., Shi, L., Li, S., Yang, Z., Standley, C., Yang, Z., ZhuGe, R., Savidge, T., Wang, X., and Feng, H. (2013) A segment of 97 amino acids within the translocation domain of *Clostridium difficile* toxin B is essential for toxicity. *PLoS One* **8,** e58634
29. Pruitt, R. N., Chambers, M. G., Ng, K. K., Ohi, M. D., and Lacy, D. B. (2010) Structural organization of the functional domains of *Clostridium difficile* toxins A and B. *Proc. Natl. Acad. Sci. U.S.A.* **107,** 13467–13472
30. Marozsan, A. J., Ma, D., Nagashima, K. A., Kennedy, B. J., Kang, Y. K.,

Arrigale, R. R., Donovan, G. P., Magargal, W. W., Maddon, P. J., and Olson, W. C. (2012) Protection against *Clostridium difficile* infection with broadly neutralizing antitoxin monoclonal antibodies. *J. Infect. Dis.* **206,** 706–713

31. Humphreys, D. P., and Wilcox, M. H. (2014) Antibodies for treatment of *Clostridium difficile* infection. *Clin. Vaccine Immunol.* **21,** 913–923
32. Orth, P., Xiao, L., Hernandez, L. D., Reichert, P., Sheth, P. R., Beaumont, M., Yang, X., Murgolo, N., Ermakov, G., DiNunzio, E., Racine, F., Karczewski, J., Secore, S., Ingram, R. N., Mayhood, T., Strickland, C., and Therien, A. G. (2014) Mechanism of action and epitopes of *Clostridium difficile* toxin B-neutralizing antibody bezlotoxumab revealed by x-ray crystallography. *J. Biol. Chem.* **289,** 18008–18021
33. Hernandez, L. D., Racine, F., Xiao, L., DiNunzio, E., Hairston, N., Sheth, P., Murgolo, N., and Therien, A. G. (2014) Broad coverage of genetically diverse strains of *Clostridium difficile* by actoxumab and bezlotoxumab as predicted by in vitro neutralization and epitope modeling. *Antimicrob. Agents Chemother.* 10.1128/AAC.04433–04414
34. Leuzzi, R., Spencer, J., Buckley, A., Brettoni, C., Martinelli, M., Tulli, L., Marchi, S., Luzzi, E., Irvine, J., Candlish, D., Veggi, D., Pansegrau, W., Fiaschi, L., Savino, S., Swennen, E., Cakici, O., Oviedo-Orta, E., Giraldi, M., Baudner, B., D'Urzo, N., Maione, D., Soriani, M., Rappuoli, R., Pizza, M., Douce, G. R., and Scarselli, M. (2013) Protective efficacy induced by recombinant *Clostridium difficile* toxin fragments. *Infect. Immun.* **81,** 2851–2860